doi: 10.15407/ujpe62.04.0311

V.E. MOISEENKO, A.V. LOZIN, M.M. KOZULIA, YU.K. MIRONOV, V.S. ROMANOV, V.G. KONOVALOV, A.N. SHAPOVAL

Institute of Plasma Physics,
National Scientific Center "Kharkiv Institute of Physics and Technology"
(1, Akademichna Str., Kharkiv 61108, Ukraine; e-mail: mikekozulya@kipt.kharkov.ua)

ALFVÉN PLASMA HEATING IN STELLARATOR URAGAN-2M

PACS 28.52.Av, 28.41.Ak

A new antenna of the crankshaft type is successfully employed in experiments on Uragan-2M. It creates and heats plasma at frequencies below the ion-cyclotron frequency. The discharge created with the antenna is "hot" during few milliseconds and then fades under strong impurity influx into plasma. The radial profiles of OV and CV optical emissions are investigated. Both are concave, especially the OV profile. This can be explained by some burnout of O^{4+} and C^{4+} ions and its transition to O^{5+} and C^{5+} ionization states near the magnetic axis. The magnetic field optimisation and the Alfvén heating allowed burning-out the light impurities prior to the discharge degradation. The experiments in support of the fusion-fission stellarator reactor concept are also carried out. The stellarator-mirror machine is modeled by switching off a toroidal field coil at Uragan-2M. The embedded mirror with lower magnetic field is created in this way. Plasma is successfully produced and heated in such a combined magnetic trap.

K e y w o r d s: radio frequency heating, stellarator, fusion-fission hybrid.

1. Introduction

Modern fusion experiments use three ways of the heating of plasma: neutral beam heating, electron cyclotron resonance (ECR) heating, and ion cyclotron radio-frequency (ICRF) heating. The Alfvén resonance heating is mainly used in small machines, although it has also a prospect to be used in a stellarator fusion reactor [1]. The energy of waves is transferred to electrons in the bulk via the Landau damping, so that fast particles are not generated. The heating uses frequencies lower than the ion cyclotron one, and the optimum heating frequency decreases, as the plasma size increases. For the reactor size machine, the frequency is in the range 1–10 MHz. The power with such frequencies could be generated with the efficiency close to 100%. The voltage on the antenna is lower than that in the ICRF heating, thus the antenna design has fewer technical problems. The theoretical background for the Alfvén plasma production and heating is under development from the 1970s. Here, the efforts of the Lausanne [2] and Sukhumi [3] groups should be mentioned. The experimental studies on the Alfvén resonance plasma heating were performed on several small devices: on stellarators Proto-Cleo in Great Britain [5], R-0 [6], Uragan-2 and Uragan-3M in the former USSR [7], and on GDT open trap (Russia) [8]. The thorough studies of Alfvén resonance heating mechanisms was performed on a TCA tokamak in Switzerland [9]. These studies were continued in Brazil on the upgraded version of a TCA tokamak (TCABR) [10]. The Alfvén resonance plasma heating was used for the plasma production in many small plasma devices of different types: It was exploited on TARA (USA) [11] and HANBIT (S. Korea) [12] open traps, in GAMMA-10 (Japan) [13], and in R-0 [6], Uragan-3 [7] and CHS (Japan) [14] stellarators. The Alfvén resonance plasma heating is used at Uragan stellarators starting from the 1970s [15] up to the present time [16].

2. Alfvén Heating

The Alfvén resonance heating is used at frequencies lower than the ion cyclotron one. It is based on the Alfvén resonance phenomenon [18,19]. In uniform plasma at low frequencies and in the ideal MHD limit (infinite plasma conductivity along the magnetic field lines), two waves can propagate: a fast magneto-sonic

wave with dispersion

$$k^2 = {k_0}^2 \varepsilon_\perp \tag{1}$$

($k_0 = \omega/c$) and the shear Alfvén wave

$$k_\parallel^2 = {k_0}^2 \varepsilon_\perp. \tag{2}$$

Here, $\varepsilon_\perp = \mathbf{k}_\perp \cdot \hat{\boldsymbol{\varepsilon}} \cdot \mathbf{k}_\perp / k_\perp^2$, $\hat{\boldsymbol{\varepsilon}}$ is the plasma dielectric tensor, $\mathbf{k}_\perp = \mathbf{k} - k_\parallel \mathbf{B}_0/B_0$, $k_\parallel = \mathbf{k} \cdot \mathbf{B}_0/B_0$, and $\mathbf{B}_0$ is the steady magnetic field.

If plasma is non-uniform in the radial direction, the shear Alfvén wave is restricted to exist at certain magnetic surfaces (Alfvén resonance surfaces), at which Eq. (2) is satisfied. Since, for given $k_\parallel$, the frequency changes continuously in the radial direction, the spectrum of a shear Alfvén wave forms the Alfvén continuum. The fast magnetosonic wave couples to the shear Alfvén wave at the Alfvén resonance position and supplies power to it [19]. If the wave energy dissipation is present in plasma, i.e. the dielectric tensor is non-Hermitian, the electromagnetic field increases at the resonant point to a finite value, and the radio frequency (RF) power is delivered to plasma. It is necessary to note that the amount of power delivered does not depend on the character of the damping processes in an Alfvén resonance vicinity. If there is no damping, the electromagnetic field diverges on the Alfvén resonance surfaces.

For Uragan-2M, the Alfvén resonance heating is theoretically studied in [20].

3. Uragan-2M

Uragan-2M [17] is a stellarator (torsatron) with the major radius $R = 170\,\text{cm}$, plasma average minor radius $r_{pl} < 24\,\text{cm}$, and toroidal magnetic field $B_0 < 2.4\,\text{T}$. It has $l = 2$ magnetic helical windings with four periods of a magnetic field $m = 4$ in the toroidal direction. The additional toroidal magnetic field is provided by sixteen toroidal magnetic coils. Four correctional coils create a vertical magnetic field for compensation of the vertical field generated by a helical winding and for the plasma column position control. Every set of coils is powered separately by the individual direct current generators. The currents creating the vertical magnetic field are used for the plasma column position adjustment in the radial direction. An increase of the current in coils creating the vertical magnetic field moves the plasma column outward, and a decrease moves it inward. The vacuum chamber has toroidal shape with a minor radius of 34 cm.

The poloidal cross-sections of the magnetic surfaces of the device have elliptic form with the ellipticity up to 2. There is practical interest in the magnetic configurations with rotational transform of $\iota/2\pi > 1/3$ in a region near the magnetic axis and $\iota/2\pi < 1/2$ for the last closed magnetic surface. In this case, the magnetic well depth is 4.3%.

4. Antennas of Uragan-2M

Two antennas are employed in this experimental series. The frame antenna is used for plasma production, and the crankshaft antenna is used for plasma heating. The RF-generators Kaskad-1 and Kaskad-2 power, respectively, the frame and crankshaft antennas. Both antennas are adjusted for the Alfvén plasma heating according to the plasma density and the magnetic field. The crankshaft-type antenna was used for the heating of plasma in a wide range of densities at Uragan-3M [23], and a similar antenna was made for the plasma heating experiments at Uragan-2M.

The antenna shapes are adjusted to the last closed magnetic surface and situated 1 cm away from it. The frame sizes are 70 cm in the toroidal direction and 50 cm in the poloidal direction. The crankshaft antenna contains three straps. The central strap is wiggled in order to facilitate the plasma production with this antenna. Both antennas are made of a stainless non-magnetic steel and are covered with a titanium nitride coating. The frame antenna circumflexes the outer part of the plasma column at the place, where the elliptic plasma cross-section is horizontally oriented. The crankshaft antenna is in the place, where the plasma cross-section ellipse is vertical. The frame antenna has a bipolar feed-through, while the crankshaft antenna is fed unipolarly.

5. Regime of Operation and Diagnostics

The optical measurements are the main diagnostics used to investigate the plasma parameters. The temporal behavior of H_α (656.2 nm), OII (372.7 nm), CIII (229.7 nm), OV (278.1 nm), and CV (227.1 nm) optical lines is recorded. All these measurements are carried out along the central chord of the vacuum chamber.

The emission intensity of the optical lines of impurities reflects the approximate highest level of the energy of plasma electrons. The existence of a certain ionization level for some certain impurity allows one to estimate the achieved energy.

The O^{4+} ion characteristics are the following: the energy necessary for obtaining the O^{4+} ion from a lower ionization state is 77.39 eV, the excitation and ionization thresholds are 72.27 eV and 113.87 eV correspondingly. For this ion, the thresholds are more than 2 times higher than for C^{2+} ion. The threshold to create C^{4+} from the previous ionization state is 64.48 eV, the excitation and ionization thresholds are 278.1 eV and 392 eV. Because of the high excitation threshold, this impurity ion can radiate efficiently only in plasma with electron temperatures higher than 100 eV.

6. Typical Discharge

The Alfvén resonance heating was attempted on Uragan-2M after its renewal in the year of 2007 [21]. In those experiments, the frame antenna was used. Some time later, the accident of vacuum oil injection into a vacuumized vessel had happened. This hampered the plasma heating.

The carried out experimental campaign at Uragan-2M torsatron is a first plasma heating campaign after a series of campaigns for the wall conditioning. The standard operation regime at Uragan-2M involves the use of the frame antenna for the pre-ionization and the crankshaft antenna for an increase of the plasma density and for the heating. Only a low power is required to initiate plasma. The anode voltage of the Kaskad-1 generator is as low as $U_{\mathrm{K1}} = 3.7\,\mathrm{kV}$, and the output power is below $P_{\mathrm{K1}} \sim$ $\sim 50\,\mathrm{kW}$. The heating frequency is $f_{\mathrm{K1}} = 5.7\,\mathrm{MHz}$. The antenna is switched-on at the time moment $t_{\mathrm{K1on}} = 1\,\mathrm{ms}$ and switched-off at the time moment $t_{\mathrm{K1off}} = 16\,\mathrm{ms}$. Kaskad-2 powers the crankshaft antenna at $f_{\mathrm{K2}} = 4.8\,\mathrm{MHz}$ from $t_{\mathrm{K2on}} = 16\,\mathrm{ms}$ to $t_{\mathrm{K2off}} = 19\,\mathrm{ms}$. The anode voltage of Kaskad-2 is as high as $U_{\mathrm{K2}} = 8.5\,\mathrm{kV}$, and the corresponding RF power is about $P_{\mathrm{K2}} \sim 300\,\mathrm{kW}$. The magnetic field is tuned to find the optimum regime. In this regime, the toroidal magnetic field is $B_0 = 3.8\,\mathrm{kG}$, and the current in the coils creating the vertical field is $I_{\mathrm{corr}} = 600\,\mathrm{A}$. The operational magnetic configuration is chosen according to the magnetic surfaces measurements [22]. All operations are provided with the neutral gas (hydrogen) pressure $P_{\mathrm{H_2}} = 1.8 \times$ $\times\, 10^{-5}$ Torr.

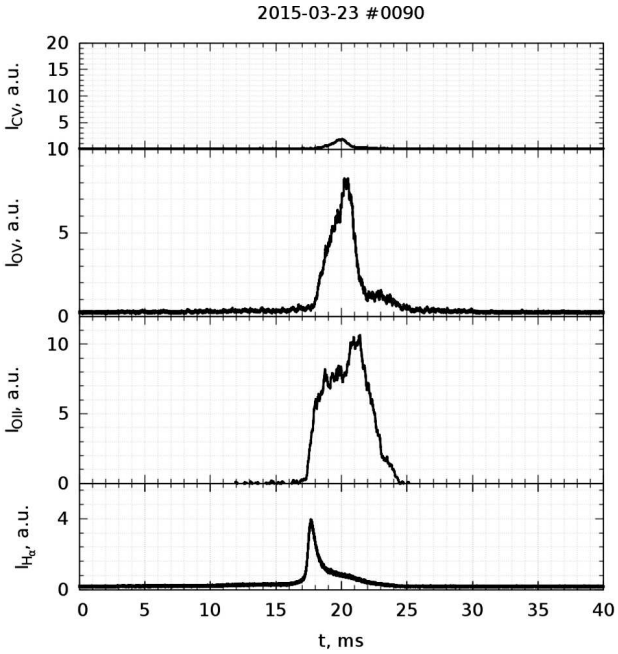

Fig. 1. Intensities of optical emission lines (a.u.) during the 40-ms standard impulse, $I_{\mathrm{corr}} = 600\,\mathrm{A}$

The frame antenna produces low-density cold plasma, which is accompanied by the emission of H_α and OII lines (Fig. 1). The molecular background noise is registered at the place of emission of the OV line. After the pre-ionization stage, the heating begins by means of the crankshaft antenna. Plasma is turned into the fully ionized state, oxygen is ionized to O^{4+} ions, and the carbon C^{4+} line emission is weak.

7. Vertical Field Influence

The vertical field compensates the parasitic magnetic field created by the helical magnetic coils and also controls a plasma column position. In the device, the vertical magnetic field is created by two sets of coils. The first compensating set of coils is fed by a current proportional to the helical winding current. Another set of correcting coils is used to tune the vertical magnetic field. An increase of the vertical magnetic field causes shifting the magnetic axes outward. In the experimental series, the vertical field is varied to find an optimum plasma column position. Its influence can be seen in Fig. 2. A decrease of

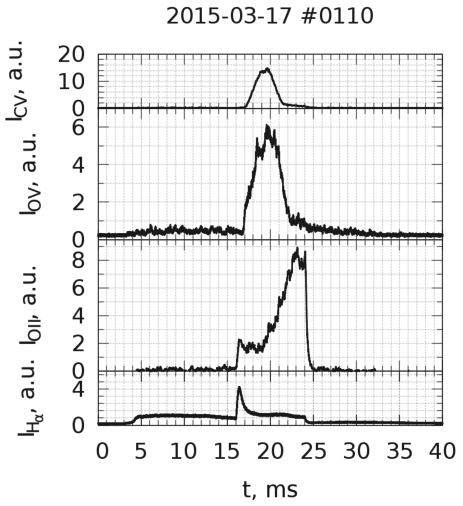

Fig. 2. Intensities of optical emission lines (a.u.) during the 40-ms impulse with a decreased vertical field, $I_{\rm corr} = 150$ A

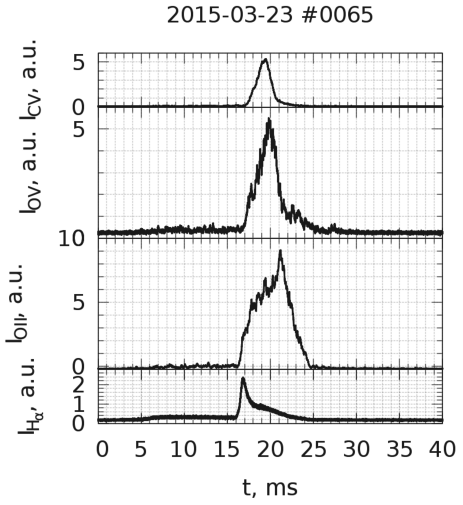

Fig. 3. Intensities of optical emission lines (a.u.) during the 40-ms impulse with a disabled toroidal coil, $I_{\rm corr} = 100$ A

the vertical field and shifting the plasma column inward improves plasma parameters. There appears the CV emission and OII burnout during the crankshaft antenna pulse. This indicates that the plasma temperature increases.

8. Experiments with Single Disconnected Toroidal Coil

On Uragan-2M, the experiments in support for the stellarator-mirror fission fusion reactor concept [24] are carried on. In this concept, a magnetic mirror is

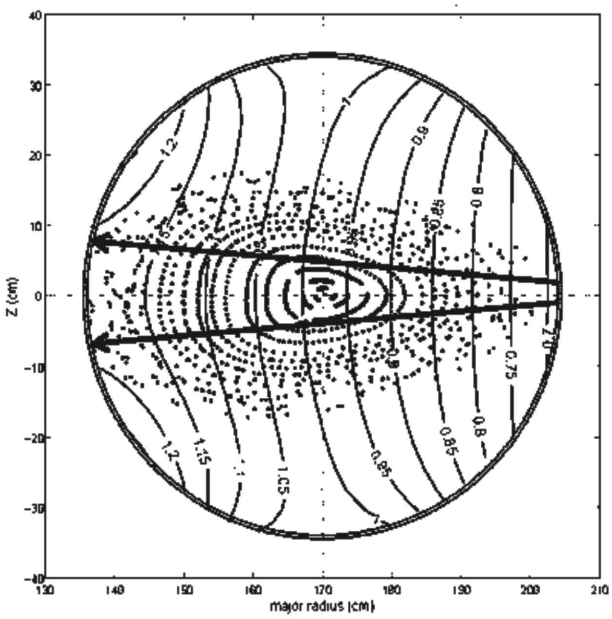

Fig. 4. Scheme of chord measurements. Arrows show the margins of the chord interval. Dots correspond to the magnetic surfaces. Vertical lines show the contours of the magnetic field modulus

embedded into a stellarator to provide the magnetic trapping of energetic sloshing (tritium) ions. The background (deuterium) plasma is warm (1–2 keV in temperature) and dense and occupies the whole plasma column. Such a combined magnetic trap could be modeled at Uragan-2M. If one toroidal magnetic field coil is switched-off, a local decrease of the magnetic field under the coil occurs. The mirror ratio of a resulted open trap is about 1.5, which is sufficient for the confinement of hot sloshing ions [25]. Under certain conditions, the nested magnetic surfaces could be arranged in a combined trap [26, 27], which is necessary for the background plasma confinement.

The numerical modeling of the Uragan-2M magnetic field configuration with one disabled toroidal coil showed the existence of closed magnetic surfaces at $k_\varphi = 0.34$. Here, k_φ is the ratio of toroidal magnetic fields on the geometrical axis induced by the helical coils to the total toroidal field. The modeling of the hybrid reactor regime is carried out with the single toroidal coil turned-off. The chosen coil is situated far from the antennas. The standard magnetic field of $B_0 = 3.7$ kG is adjusted to the new regime, by decreasing the vertical correcting field coil current down to $I_{\rm corr} = 100$ A. Kaskad-1 with the anode volt-

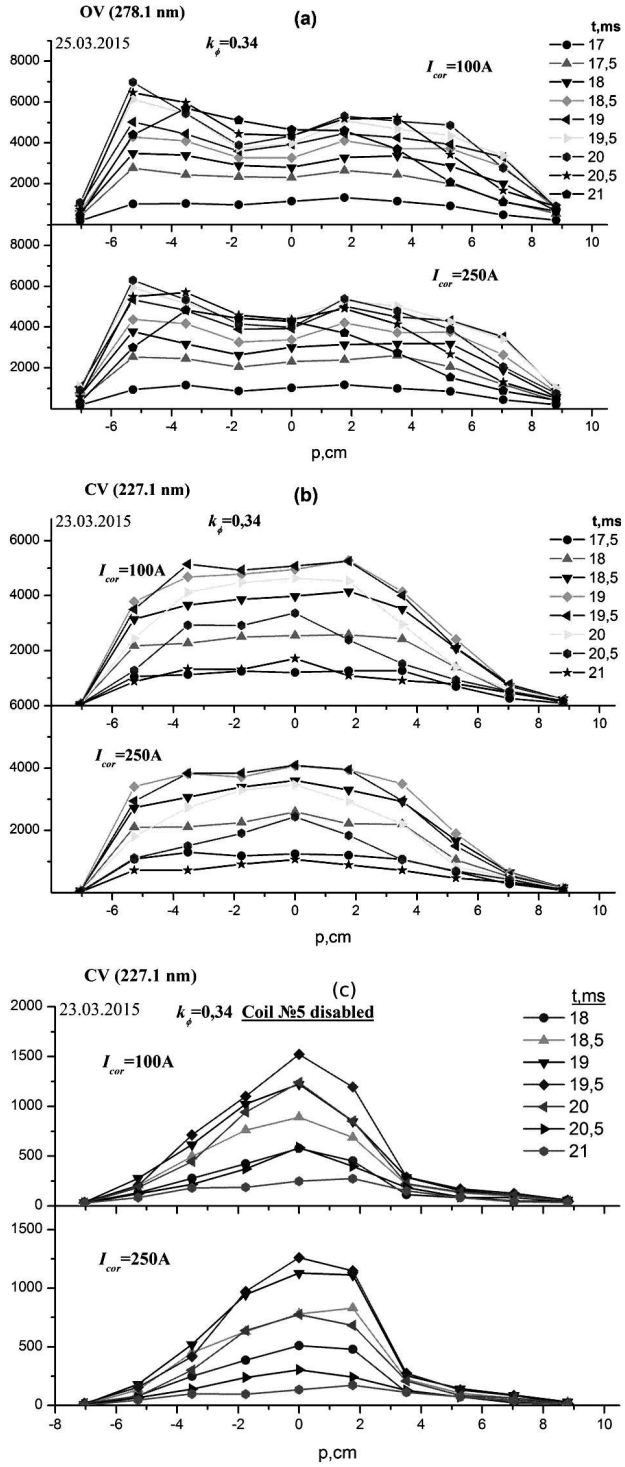

Fig. 5. Chord disributions timelaps of OV (a), CV in the full magnetic configuration (b), and CV in the regime with a single toroidal coil disabled (c)

age $U_{\mathrm{K1}} = 3.7\,\mathrm{kV}$ powers the frame antenna, which provides the stable pre-ionization. The duration of Kaskad-1 is increased in comparison with the standard regime: $t_{\mathrm{K1on}} = 1\,\mathrm{ms}$, $t_{\mathrm{K1off}} = 16\,\mathrm{ms}$. Kaskad-2 has anode voltage decreased down to $U_{\mathrm{K2}} = 8\,\mathrm{kV}$ to minimize the risk of arcing the crankshaft antenna at the feed-through powers between time moments $t_{\mathrm{K2on}} = 16\,\mathrm{ms}$, $t_{\mathrm{K2off}} = 24\,\mathrm{ms}$. The neutral gas pressure is also decreased comparing to the standard regime as a result of the discharge optimization $P_{\mathrm{H_2}} = 9.7 \times 10^{-6}\,\mathrm{Torr}$.

The plasma production and confinement in such an arrangement are preliminarily assessed experimentally on Uragan-2M. The light impurity radiation barrier is passed at the beginning of the discharge (see Fig. 3). Highly ionized states of impurities, e.g., O^{4+} and C^{4+}, are created. After few milliseconds, the discharge fades owing to the contamination by impurities. The highly ionized light impurity emissions are weaker than in the experiment without switching-off one coil of the toroidal field. The chord distributions of CV (see Fig. 5) are peaked, which indicates almost no burnout of O^{4+} and C^{4+}. The distributions are narrower, which could be explained by a smaller minor radius of the plasma column. The latter is in agreement with calculations of the magnetic configuration [26]. The comparison with the impulse in Fig. 2 shows some shortening of the high temperature stage of the discharge (see Fig. 3), which is accompanied by the O^{4+} and C^{4+} emissions.

9. Radial Distributions

Shot-by-shot measurements of chord distributions of the OV and CV emissions are made. The scheme of measurements is presented in Fig. 4. The chords cover only the central area of the plasma column. The results of measurements are presented in Fig. 5. The distribution of the OV emission is concave. This may be explained by some burnout of O^{4+} ions and their transition to the O^{5+} ionization state near the magnetic axis. The CV emission distribution is flattened. This means that the radial profile of the emission is concave only slightly.

10. Conclusion

A new antenna of the crankshaft type is successfully employed in experiments on Uragan-2M. It creates and heats plasma at frequencies below the ion-cyclotron frequency. The discharge sustained by the

antenna is "hot" during few milliseconds and then fades under a strong impurity influx into plasma. The radial profiles of OV and CV optical emissions are investigated. Both are concave, especially the OV profile. This may be explained by some burnout of O^{4+} and C^{4+} ions and by their transition to O^{5+} and C^{5+} ionization states near the magnetic axis.

The experiments in support of the fusion-fission stellarator reactor concept are carried out. The stellarator-mirror machine is modeled by switching-off the toroidal field coil on Uragan-2M. The embedded mirror with lower magnetic field is created in this way. Plasma is successfully produced and heated in such a combined magnetic trap.

1. J. Vaclavik, K. Appert. Theory of plasma heating by low frequency waves: Magnetic pumping and Alfvén resonance heating. *Nucl. Fusion* **31**, 1945 (1991) [DOI: 10.1088/0029-5515/31/10/013].
2. O.P. Fesenyuk, Ya.I. Kolesnichenko, V.V. Lutsenko, R.B. White, Yu.V. Yakovenko. Alfvén continuum and Alfvén eigenmodes in the National Compact Stellarator Experiment. *Phys. Plasmas* **11**, 5444 (2004) [DOI: 10.1063/1.1806136].
3. A.G. Elfimov, S.N. Lozovskij, V.V.Dorokhov. Alfvén heating of a plasma with an axial homogeneous current. *Nucl. Fusion* **24**, 609 (1984) [DOI: 10.1088/0029-5515/24/5/007].
4. K. Appert, G.A. Collins, F. Hofmann, R. Keller, A. Lietti, J.B. Lister, A. Pochelon, L. Villard. Observations of toroidal coupling for low-n Alfvén modes in the TCA tokamak. *Phys. Rev. Lett.* **54**, 1671 (1985) [DOI: 10.1103/PhysRevLett.54.1671].
5. S.N. Golovato, J.L. Shohet, J.A. Tataronis. Alfvén-wave heating in the Proto-Cleo stellarator. *Phys. Rev. Lett.* **37**, 1272 (1976) [DOI: 10.1103/PhysRevLett.37.1272].
6. R.A. Demirkhanov, A.G. Kirov, G.I. Astapenko *et al.* Plasma heating and current drive by Alfvén waves. In: *9th Int. Conf. on Plasma Phys. and Contr. Nucl. Pus. Res., IAEA, Vienna*, vol. 2, 91 (1983).
7. O.M. Shvets, I.A. Dikij, S.S. Kalinichenko *et al.* Absorption of Alfvén waves and plasma production in the OMEGA and URAGAN-3 toroidal devices. *Nucl. Fusion* **26**, 23 (1986).
8. V.E. Moiseenko, A.A. Ivanov, A.V. Anikeev, P.A. Bagryansky. *12th Topical Conf. On RF Power in Plasmas, Savannah, GA, AIP Conference Proceedings, AIP, New York*, p. 479 (1997).
9. G. Besson, A. de Chambrier, G.A. Collins, B. Joye, A. Lietti, J.B. Lister, J.M. Moret, S. Nowak, C. Simm, H. Weisen. A review of Alfvén wave heating. *Plasma Phys. Control. Fusion* **28**, 1291 (1986) [DOI: 10.1088/0741-3335/28/9A/008].
10. L.F. Ruchko, E. Lerche, R.M.O. Galvão, A.G. Elfimov, I.C. Nascimento, W.P. de Sá, E. Sanada, J.I. Elizondo, A.A. Ferreira, S. Saettone, J.H.F. Severo, V. Bellintani, O.C. Usuriaga. The analysis of Alfvén wave current drive and plasma heating in TCABR tokamak. *Braz. J. Phys.* **32**, 57 (2002) [DOI: 10.1590/S0103-97332002000100012].
11. S.N. Golovato, K. Brau, J. Casey, J. Coleman, M.J. Gerver, W. Guss, G. Hallock, S. Horne, J. Irby, R. Kumazawa, J. Kesner, B. Lane, J. Machuzak, T. Moran, R. Myer, R.S. Post, E. Sevillano, D.K. Smith, J.D. Sullivan, R. Torti, L. Wang, Y. Yasaka, X.Z. Yao, J. Zielinski. Plasma production and heating in a tandem mirror central cell by radio-frequency waves in the ion cyclotron frequency range. *Phys. Fluids* **31**, 3744 (1988) [DOI: 10.1063/1.866893].
12. M. Kwon, J.G. Bak, K. Choh *et al.* Recent results of the HANBIT mirror device. *Fusion Sci. Technol.* **43** (1T), 23 (2003).
13. M. Ichimura, S. Tanaka, C. Nakagawa *et al.* High-density plasma production with fast Alfvén waves in the GAMMA 10 tandem mirror. *Fusion Sci. Technol.* **39**, 167 (2001).
14. K. Nishimura, T. Shoji, and CHS Group. Experiment on RF plasma production in CHS. *Stellarator Physics. Proc. 7th Int. Workshop Oak Ridge, TN, 1989, IAEA-TECDOC-558, IAEA, Vienna, 265* (1990).
15. A.G. Dikij, S.S. Kalinichenko, A.A. Kalmykov, I.I. Konovalov, S.S. Ovchinnikov, O.S. Pavlichenko, V.K. Pashnev, A.S. Slavnyi, V.A. Suprunenko, V.F. Tarasenko, V.T. Tolok, O.M. Shvets. RF plasma heating in the Uragan stellarator. I. Wave launching and plasma heating. *Plasma Phys.* **18**, 577 (1976) [DOI: 10.1088/0032-1028/18/8/001].
16. V.E. Moiseenko, V.L. Berezhnyj, V.N. Bondarenko, P.Ya. Burchenko, F. Castejen, V.V. Chechkin, V.Ya. Chernyshenko, M.B. Dreval, I.E. Garkusha, G.P. Glazunov, L.I. Grigor'eva, D. Hartmann, C. Hidalgo, R. Koch, V.G. Konovalov, V.D. Kotsubanov, Ye.D. Kramskoi, A.E. Kulaga, A.V. Lozin, A.I. Lyssoivan, V.K. Mironov, I.N. Mysiura, R.O. Pavlichenko, V.K. Pashnev, V.S. Romanov, A.N. Shapoval, A.I. Skibenko, A.S. Slavnyi, E.L. Sorokovoy, Yu.S. Stadnik, V.S. Taran, V.I. Tereshin, V.S. Voitsenya. RF plasma production and heating below ion-cyclotron frequencies in Uragan torsatrons. *Nucl. Fusion* **51**, 083036 (2011) [DOI: 10.1088/0029-5515/51/8/083036].
17. O.S. Pavlichenko for the U-2M group. First results from the 'URAGAN-2M' torsatron. *Plasma Phys. Control. Fusion* **35**, B223 (1993) [DOI: 10.1088/0741-3335/35/SB/018].
18. V.V. Dolgopolov, K.N. Stepanov. Cerenkov absorption of Alfvén waves and of fast magneto-acoustic waves in an inhomogeneous plasma. *Nucl. Fusion.* **5**, 276 (1965) [DOI: 10.1088/0029-5515/5/4/003].
19. J. Tataronis, W. Grossman. Decay of MHD waves by phase mixing. *Z. Phys.* **261**, 203 (1973) [DOI: 10.1007/BF01391913].
20. V.E. Moiseenko, Ye.D. Volkov, V.I. Tereshin, Yu.S. Stadnik. Alfvén resonance heating in Uragan-2M torsatron. *Plasma Phys. Reports* **35**, 828 (2009) [DOI: 10.1134/s1063780x09100043].
21. V.I. Tereshin *et al.* First results of the renewed Uragan-2M torsatron. *35th EPS Conference on Plasma Phys. Hersonissos, 9–13 June 2008, ECA*, **32**, 1.061 (2008).

22. G.G. Lesnyakov, D.P. Pogozhev, Yu.K. Kuznetsov *et al.* Studies of magnetic surfaces in the Uragan-2M torsatron. *Contributed Papers of 23rd EPS Conf. on Contr. Fusion and Plasma Phys., Kiev,* **20** C, Part II (b025), 547 (1996).
23. V.V. Plyusnin, V.E. Moiseenko, A.I. Lysoivan, S.V. Kasilov, A.I. Zhukov, N.I. Nazarov, E.D. Volkov, K.N. Stepanov, O.S. Pavlichenko. ICRF plasma production and heating in the URAGAN-3M torsatron. *International Atomic Energy Agency, Vienna (Austria)*, 95 (1997).
24. V.E. Moiseenko, V.G. Kotenko, S.V. Chernitskiy *et al.* Research on stellarator–mirror fission–fusion hybrid. *Plasma Phys. Control. Fusion* **56**, 094008 (2014).
25. V.E. Moiseenko, O. Ågren. Stellarator-mirror hybrid with neutral beam injection. *Fusion Science and Technology* **63** (1T), 119 (2013).
26. V.G. Kotenko, V.E. Moiseenko, O. Ågren. Magnetic field of a combined plasma trap. *AIP Conf. Proc.* 1442, 167 (2012) [DOI: 10.1063/1.4706866].
27. G.G. Lesnyakov, A.N. Shapoval, S.P. Gubarev, M.S. Zolototrubova, G.P. Opaleva, M.N. Makhov, V.G. Kotenko, V.E. Moiseenko, V.S. Voitsenya. Magnetic surfaces of stellarator-mirror hybrid in the Uragan-2M torsatron. *Problems of Atomic Science and Technology* **83** (1), 57 (2013).

Received 27.11.15

В.Є. Моісеєнко, А.В. Лозін,
М.М. Козуля, Ю.К. Міронов, В.С. Романов,
В.Г. Коновалов, А.Н. Шаповал

АЛЬФВЕНІВСЬКИЙ НАГРІВ
ПЛАЗМИ В СТЕЛАРАТОРІ УРАГАН-2М

Р е з ю м е

Нова антена колінвального типу успішно застосовується в експериментах на Урагані-2М. Вона створює та нагріває плазму на частотах, нижчих за іонно-циклотронну частоту. Антена створює "гарячий" розряд лише на декілька мілісекунд, який згасає разом з сильним потоком домішок у плазму. Досліджено радіальні профілі оптичного випромінювання OV та CV. Обидва профілі впалі, особливо профіль OV. Це може бути пояснено вигорянням іонів O^{4+} і C^{4+} та їхнім переходом до станів іонізації O^{5+} і C^{5+} поблизу магнітної осі. Оптимізація магнітного поля й альфвенівський нагрів дозволили досягти вигоряння легких домішок до початку деградації розряду. Було проведено експерименти щодо підтримки концепції гібридного реактора на основі стеларатора. Стелараторно-пробкотронний гібрид моделюється вимкненням однієї котушки тороїдального поля Ураган-2М. Таким чином створюється вбудований пробкотрон зі зниженим магнітним полем. Плазма успішно створюється та утримується в такій комбінованій пастці.